PERGAMON

International Journal of Mechanical Sciences 44 (2002) 103–122

International Journal of MECHANICAL SCIENCES

www.elsevier.com/locate/ijmecsci

Simulation of springback

K.P. Li[a], W.P. Carden[b], R.H. Wagoner[a,*]

[a] Department of Materials Science and Engineering, The Ohio State University, 177 Watts Hall, 2041 College Road, Columbus, OH 43210-1179, USA

[b] Monteagle Corporation, Birmingham, Alabama, USA

Received 16 May 2000; received in revised form 2 July 2001

Abstract

Springback, the elastically-driven change of shape of a part after forming, has been simulated with 2-D and 3-D finite element modeling. Simulations using solid and shell elements have been compared with draw-bend measurements presented in a companion paper. Plane-stress and plane-strain simulations revealed the dramatic role of numerical tolerances and procedures on the results. For example, up to 51 integration points through the sheet thickness were required for accuracy within 1%, compared with 5–9 typically acceptable for forming simulations. Improvements were also needed in the number of elements in contact with the tools, and in the numerical tolerance for satisfying equilibrium at each step. Significant plastic straining took place in some cases upon unloading; however the choice of elastic–plastic unloading scheme had little effect on the results. While 2-D simulations showed good agreement with experiments under some test conditions, springback discrepancies of hundreds of percent were noted for one alloy with sheet tension near the yield stress. 3-D simulations provided much better agreement, the major source of error being identified as the presence of persistent anticlastic curvature. Most of the remaining deviation in results can be attributed to inaccuracies of the material model. In particular, the presence of a Bauschinger effect changes the results markedly, and taking it into account provided good agreement. Shell elements were adequate to predict springback accurately for R/t greater than 5 or 6, while solid elements were required for higher curvatures. As R/t approaches 2, springback simulated with solid elements tends to disappear, in agreement with measurements presented in the companion paper and in the literature. © 2002 Elsevier Science Ltd. All rights reserved.

Keywords: Springback; Sheet metal forming; Anticlastic curvature; DQSK steel; 6022-T4 aluminum; HSLA steel; Draw-bend tests; Plastic anisotropy; Finite element modeling; Integration points; Bauschinger effect; Shell elements; Solid elements

* Corresponding author. Tel.: +1-614-292-2079; fax: +1-614-292-6530.
E-mail address: wagoner.2@osu.edu (R.H. Wagoner).

PII: S0020-7403(01)00083-2

Nomenclature

h	arc height at the center of the strip
N_{EL}	number of elements along the length of sheet strip
N_{IP}	number of integration points through the thickness of sheet strip
F_b	actual back force
F_y	yield force
$\overline{F_b}$	normalized back force
F_f	actual front force
m	mixed hardening factor
R	tool radius
R_a	anticlastic radius of curvature on the curl region
R', θ_1	radius and corresponding angle for the region of sheet strip that has undergone only bending
r', θ_2	radius and corresponding angle for the region of sheet strip that has undergone both bending and straightening.
t	sheet thickness
w	arc width of the sheet strip cross section
θ	overall springback angle of sheet strip
κ_a	anticlastic curvature on the curl region
$\langle\sigma\rangle$	standard deviation
μ	friction coefficient

1. Introduction

As lead times are shortened and materials of higher strength are used in manufacturing, the simulation of springback following sheet forming is essential for designing tooling and processes. Traditional trial-and-error methods are time-consuming and expensive, while empirical rule-based adjustments for springback [1] are not usually applicable to complex geometries or materials without a large database of experience.

Early analytical solutions for springback of plane stress, pure bending with large R/t (radius of curvature/thickness) springback were established for elastic-perfectly plastic material response [2], and were extended to plane-strain pure bending [3], and initially curved cases [4]. Further developments include solutions for plane-strain bending with superimposed tension for arbitrary R/t [5–13] and for plane-stress bending of narrow strips [14]. Reviews of pre-1950s developments have been presented [15,16], as have more recent analytical springback methods and approaches [17,18].

Non-finite-element analytical methods have been applied to springback in die forming, often with limitations to pure bending, as appropriate for U-bending [19], flanging [20], sidewall curl [21], repeated bending unbending [22,23] or stamping with deformable tools [24]. These analyses rely on radii of curvature during the forming operation established by geometrical considerations of the dies, but do not usually solve explicitly for such shapes consistent with the material mechanics and contact/friction with the tools. With superimposed tension, these methods may be applied to plane-strain draw die forming [25–27] with gentle tooling curvatures. Such methods have also been applied to stretch bending of channels [7,28] or draw bending of top-hat sections [29].

With the rapid increase in computation power, finite element methods (FEM) for analyzing and predicting springback have become more attractive. Recent benchmark tests and accompanying papers [30–33,94] illustrate the state of the art in predicting springback with FEM. In particular, the 1993 benchmark [30] represents a flanged channel forming operation that was simulated by many commercial and special-purpose programs with widely varying results. This result was surprising in view of the reliability developed in forming simulations by that period.

FEM simulations of springback are much more sensitive to numerical tolerances than are forming simulations [34–37], including effects of element type [38], integration scheme [36–41], and unloading scheme [9,36,42]. Because of the inherent numerical sensitivity, implicit schemes for both loading and unloading (i.e. implicit/implicit) have been popular [35,36,38,43,44], as well as attempts to link dynamic explicit simulations of forming operations (upon which many commercial programs are based) to static implicit simulations of springback [39,34,45,46]. Nearly every possible approach to simulating springback has been recently reported as successful, including explicit/explicit [47], static explicit/static explicit [48], and even one-step methods [49]. Hybrid approaches have been developed for post-processing of forming FEM results for springback [50] and for optimizing die design by iterating with analysis [51–54].

Springback is also sensitive to a range of material and process parameters, such as strain hardening [27–29,55], evolution of elastic properties [56,57], elastic and plastic anisotropy [56] and the presence of a Bauschinger effect [5,10,23,29,40,50,58,59].

In order to investigate the physical and numerical sensitivity of sheet springback simulations, draw-bend tests were analyzed using finite element modeling. The draw-bend test was chosen as a well-characterized example of a forming operation that produces springback similarly to industrial press forming operations. The test mimics closely the mechanics of deformation of sheet metal as it is drawn, stretched, bent, and straightened over a die radius entering a typical die cavity. As such, it represents a wide range of sheet forming operations, but has the advantage of simplicity. The tooling and specimen may be represented as two-dimensional and, more importantly, the sheet tension may be controlled directly and accurately. In press forming operations, the sheet tension, which dominates springback effects, depends on complicated and largely unknown interactions among friction, drawbead configuration, blank holder forces and displacements, and material characteristics. For this reason, it is difficult to identify sources of error when comparing springback simulations and industrial forming operations.

2. Finite element modeling—numerical effects

FEM was carried out using a variety of elements (beam, shell, solid) and either the commercial program ABAQUS (versions 5.7 and 5.8.14) [60] or the SHEET family of research programs [61–75] (including SHEET-S and SHEET-3). Details of the element formulations and numerical procedures employed in these programs are available in the references cited. After careful control of numerical tolerance, mesh size, and integration strategy, the results were indistinguishable among the programs using the same element, so no further distinction will be made here. (The SHEET programs do not have a released solid element, so all solid simulations were conducted only with

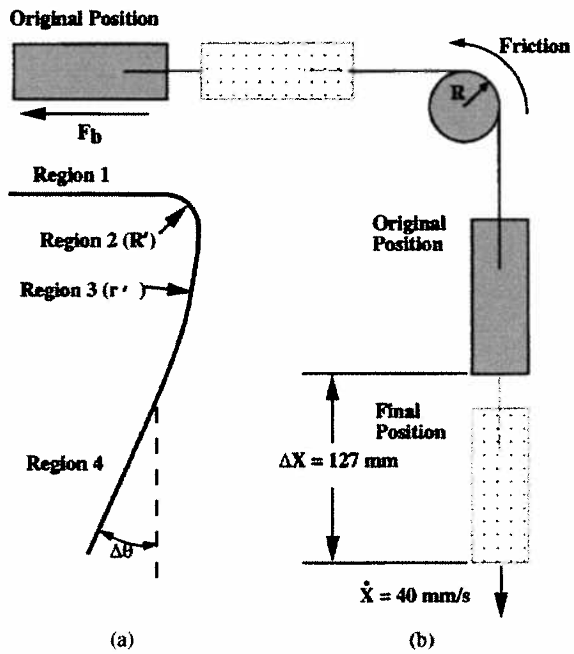

Fig. 1. Draw/bend test geometry: (a) specimen shape after unloading; and (b) original and final shapes during testing.

ABAQUS. Conversely, ABAQUS does not have a plane-strain beam element, so such simulations were conducted only with SHEET-S.)

Except as noted, all simulations were carried out using von Mises plasticity and stress–strain curves measured in uniaxial tension and fit according to procedures described elsewhere [76]. Standard friction coefficients corresponding to the various lubrication conditions are shown on each simulation. These agree approximately to those generated by comparing simulated and measured front and back forces, but the ones used in the simulations were not varied from material to material. The sensitivity of simulated springback to friction coefficient is presented.

The physical problem is sketched in Fig. 1. The starting configuration, shaded, is shown in Fig. 1b. There are three major steps in the simulation: (1) the back force F_b is applied at the upper grip while the lower grip is held immobile ($\Delta X = 0$), (2) while maintaining the back force F_b, the lower grip is displaced at a constant rate of 40 mm/s, and (3) external forces from tools and grips are removed according to an unloading scheme to observe springback. Regions 1 and 4 of the mesh (Fig. 1) remain straight throughout all steps while Regions 2 and 3 undergo bending and bending/unbending, respectively.

The first simulations used numerical parameters typical of those in forming analysis: a uniform mesh consisting of 150 plane-stress elements (for $R = 9.5$ mm) and five integration points through the thickness, Fig. 2. The results showed negative springback for sheet tensions near the material yield stress, contrary qualitatively to all experimental observations. A numerical sensitivity study [36,38,77] was undertaken with respect to contact conditions, equilibrium tolerance, element size, and integration strategy, as summarized below. Fig. 2 compares the first results to those eventually obtained with optimized numerical conditions.

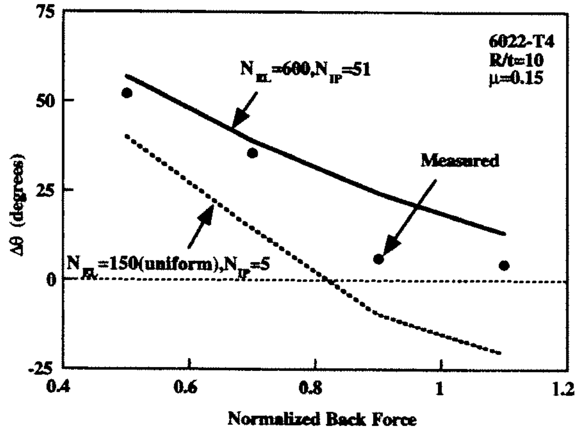

Fig. 2. Effect of numerical choices on springback prediction results.

Reliable results were obtained for all cases using a nonuniform mesh consisting of 600 elements along its length: 78 elements × 2.6 mm original length in Region 1, 60 elements × 2.8 mm in Region 4, and 452 elements × 0.31 mm in Regions 2 and 3. (As drawing proceeds, nodes flow from Region 2 to Region 3, but Regions 1 and 4 do not come into contact with the tool.) The turning angle for each element in contact with the tools in this mesh is 1.9°, much smaller than the 10° recommended for forming operations [78]. However, this mesh also gave satisfactory results, within 1% error, for a tool radius of 32 mm, where the turning angle per element is 5.5°. Mesh sensitivity was investigated using meshes scaled from this one to obtain total element numbers of 150, 300, 600, 900, 1200, and 2400.

The initial finite element mesh is in all cases based on an assumed stress-free state corresponding to the configuration shown in Fig. 1. This unloaded starting point neglects the residual stresses arising from the simple bending of the sheet around the tooling to conform to it and to form a 90° included angle initially. In order to assess the magnitude of error that this starting state represents, finite element simulations were carried out to represent the simple bending to a radius of 8–10 mm, then unloading from this state, and finally stress relieving (via a viscous creep law). Relieving of the internal stresses produced an angular change of less than 0.3°. This is less than the numerical uncertainty and experimental scatter of the results.

The sensitivity of springback results to the number of integration points through the shell thickness was even more dramatic and contrary to typical forming practice. As shown in Fig. 3, many integration points are required to obtain springback results within 1% of the limiting case (with sufficient integration points that springback angle no longer changes with additional points). Although Fig. 3 shows that for two cases the minimum number of integration points is 21 or 35, depending on back force, 51 integration points were required to ensure springback numerical accuracy within 1% of the large-number limit for all of the springback cases simulated.

Springback analysis is generally composed of two steps: loading (forming) and unloading (springback). For the unloading procedure, two methods are typically reported. One is the so-called contact release method [79], which is the most commonly used method in commercial programs such as DYNA3D or ABAQUS. During springback, all the external forces, including the contact restraint forces, are reduced gradually to zero. The contact constraint is transformed into force boundary conditions so that there is no contact treatment needed. An alternate method [80,81], may be called the

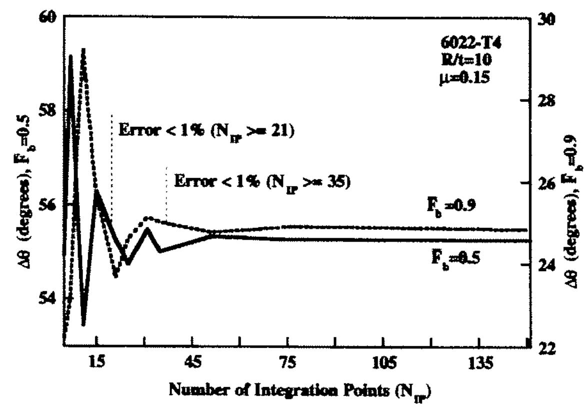

Fig. 3. Convergence of springback results with increasing number of through-thickness integration points.

forming inversion method. It inverts the loading (forming) process, and is computationally expensive but perhaps more realistic physically because of the satisfaction of contact conditions throughout the unloading step.

To test the importance of the unloading strategy, three loading schemes were implemented in SHEET-S, Fig. 4. Schemes 1 and 2 consist of two steps while Scheme 3 is accomplished in one step. The schemes can be summarized as follows:

- For Scheme 1, the springback analysis reverses the process of forming. Hence the stretching force at the end node of the sheet, where the displacement is imposed, is released first with the tool contact in place. The contact between the sheet and the cylinder disappears at the end of this step. A nearly constant moment distribution is obtained at the intermediate configuration (Fig. 5). The second step consists of freeing the end node by reducing the nodal forces (transverse force and moment) to zero.
- For Scheme 2, the contact constraint is removed by transforming the contact boundary condition into an equivalent force boundary condition and reducing these forces to zero. During this step, there is no real contact treatment: the process is a purely numerical one of force reduction. The moment distribution along the sheet at the end of this step is quite different from Scheme 1, Fig. 4b, indicating that the paths are distinct. In the final unloading, the end node is freed by reducing the nodal forces (tension, transverse force and moment) to zero.
- For Scheme 3, the contact equivalent forces and the nodal forces are proportionally reduced to zero during one step, with no contact treatment. (This is the procedure implemented in ABAQUS.)

While the computation time differs for the three schemes (Scheme 1 requires much more CPU time, and Scheme 2 is somewhat more efficient than Scheme 3), and the paths are different, Fig. 1a shows that the resulting springback shapes vary negligibly. Less than 0.2° of springback difference (out of 26.5° total) is obtained, which is smaller than other numerical tolerances.

The effective equivalence of the unloading schemes is surprising in view of the importance of plasticity during the springback step, Fig. 5. As shown, the residual stress distributions are significantly different, and these distributions correspond to a difference of 10° of springback between elastic–plastic and purely elastic unloading, the purely elastic case showing more springback. This

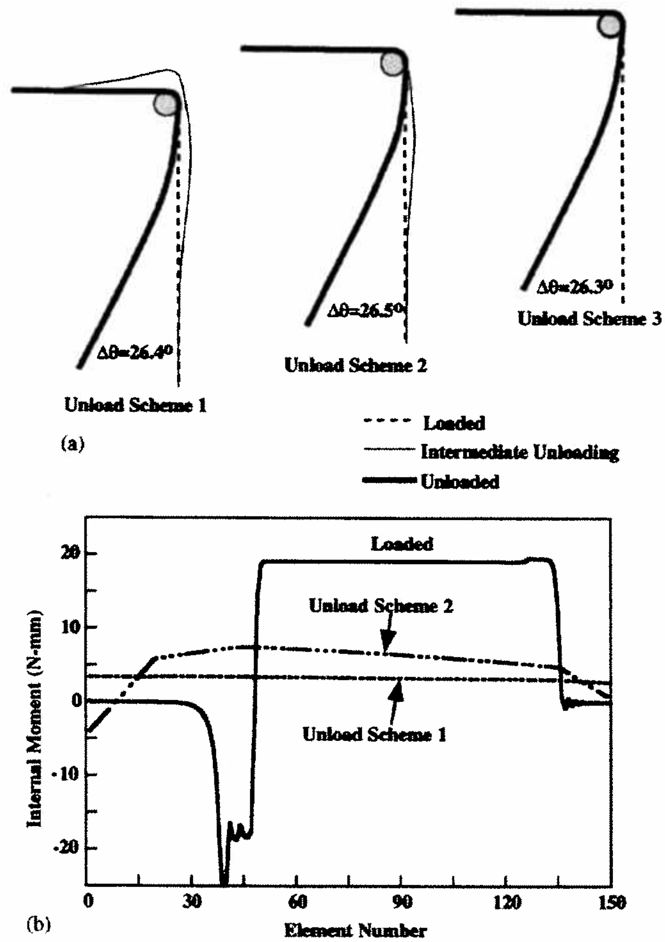

Fig. 4. (a) Intermediate and final shapes; and (b) Intermediate internal moments as simulated using two unloading schemes.

finding calls into question the common procedure of treating springback as a purely elastic process, either in concept [82,83] or by finite element implementation [84,85]. To summarize, while the unloading process requires elastic–plastic simulation for accuracy, the choice of how the unloading scheme is implemented has little effect on the result.

All simulations reported in the next section make use of the numerical findings reported above. Each simulation uses a mesh of 600 elements along the length, 51 integration points through the thickness, elastic–plastic unloading, and unloading Scheme 3.

3. Finite element modeling—physical effects

Once numerical tolerance and procedures have been established, meaningful comparisons between measurements and simulations can be attempted.

As shown in Fig. 1, the final specimen shape can be defined by two radii of curvature, R' and r', corresponding to two angles, θ_1 and θ_2. R' and θ_1 are the unloaded values corresponding to Region 2

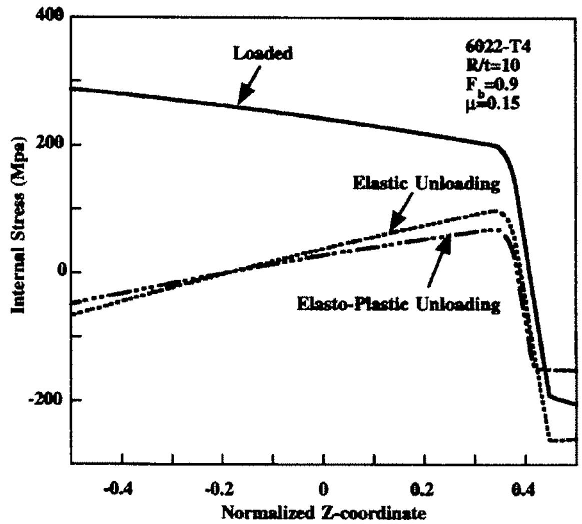

Fig. 5. Effect of elastic–plastic unloadings on the loaded and residual stress distribution.

of the strip, which remains in contact with the tool at the end of the test (before unloading), and which has undergone only bending, not straightening. r' and θ_2 correspond to Region 3, which has been drawn over the tool and which has undergone bending and straightening. The angular and curvature measures are related by fixed arc lengths of $R\pi/2$ (tool contact length) and 127 mm (the driving actuator displacement), respectively. The springback angles are the changes of these measures upon unloading:

$$\Delta\theta_1 = \theta_1 - \theta_1^{\text{loaded}} = \theta_1 - \pi/2 = \pi/2(R/R' - 1), \tag{1}$$

$$\Delta\theta_2 = \theta_2 - \theta_2^{\text{loaded}} = \theta_2 - 0^{\circ} = 127\ \text{mm}/r', \tag{2}$$

$$\Delta\theta = \Delta\theta_1 + \Delta\theta_2. \tag{3}$$

The change of θ_1 ($\Delta\theta_1$ is generally negative) represents relaxation from a single bend to conform to the tool radius while θ_2 corresponds to a region of straightening from this radius. $\Delta\theta_2$, generally positive, is a measure of "sidewall curl" [18,86] in industrial channel forming.

Fig. 6 compares the three measured and simulated springback angles for one value of tool radius and lubrication condition. At low normalized back forces, less than 0.8 times the force to yield the strip in tension, all three plane-stress simulated angles are in good agreement with the measured ones. For normalized back forces greater than 0.8, there is a sudden departure of the agreement, although the values appear to begin converging at yet higher back forces. The discrepancy for a normalized back force of 0.9 is very significant, the error for $\Delta\theta$ being several times the measured value of $\Delta\theta$. Fig. 6 also shows that the agreement or disagreement between simulations and measurements lies largely in $\Delta\theta_2$, the component angle corresponding to the sidewall curl, Region 3. Because the experimental scatter for measuring $\Delta\theta$ is much less than in deconvoluting it to obtain θ_1 and θ_2, the remaining comparisons will be provided in terms of $\Delta\theta$. It is important to keep in mind that the variation of $\Delta\theta$ is dominated by the action in Region 3.

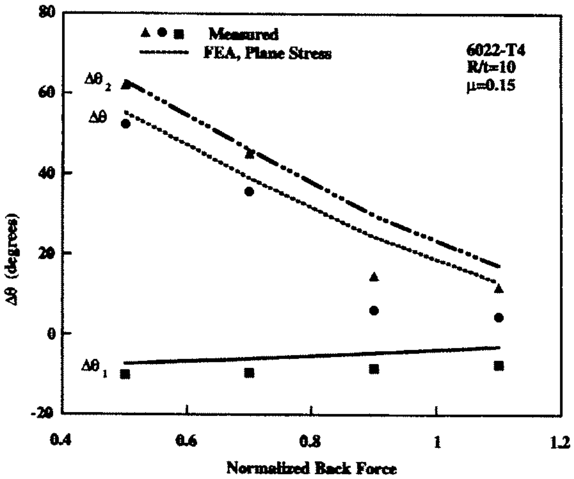

Fig. 6. Comparison of three springback angles from measurements and plane-stress simulations for 6022-T4 aluminum.

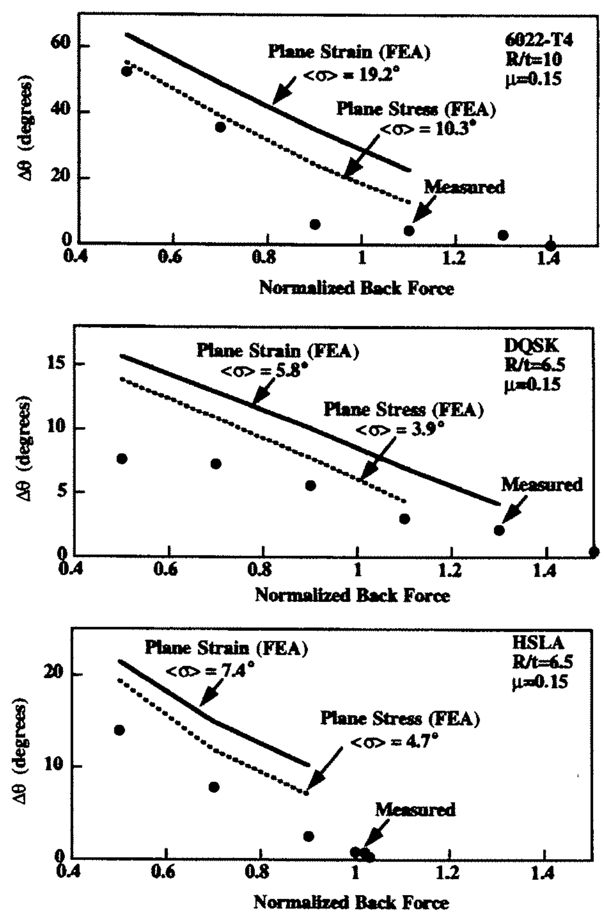

Fig. 7. Comparison of total springback angle from measurements and 2D simulations.

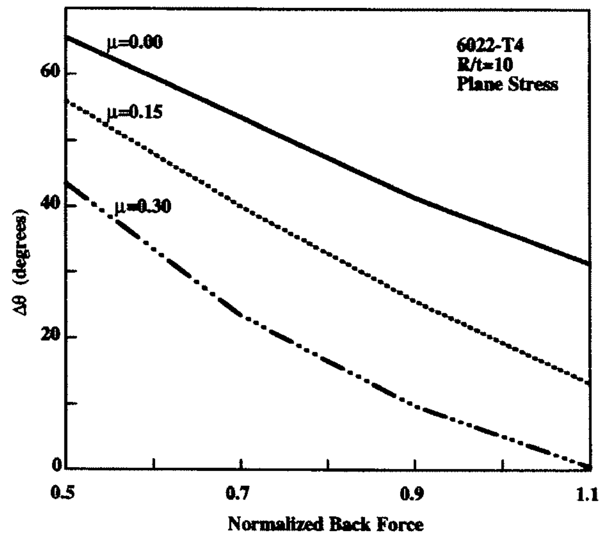

Fig. 8. Role of friction on springback angle, from plane-stress simulations.

The 2-D simulations and measurements of $\Delta\theta$ for all three tested alloys are summarized in Fig. 7 for a common tool radius of 9.5 mm and a friction coefficient of 0.15 (corresponding to the lubricated, fixed tool). The plane-strain simulated angles are in marked disagreement with measurements over the entire range of back forces, in spite of strip width/thickness ratios of 35–55. The reason for this inconsistency will be discussed in terms of anticlastic curvature below. Only the aluminum specimens (which have original thickness of 0.91 mm versus 1.5 mm for the steels) showed a marked departure between simulations and measurements as back force varied, with the appearance of a sudden jump followed by a plateau as back force increased.

The standard deviations shown in Fig. 7 and subsequently are computed on the basis of simulated and measured springback angles as follows:

$$\langle\sigma\rangle = \sqrt{\frac{\sum_{i=1}^{N}(\Delta\theta^i_{\text{measured}} - \Delta\theta^i_{\text{simulated}})^2}{N}}, \tag{4}$$

where N is the number of measurements and simulations for various back forces shown on each figure.

In order to investigate the large springback discrepancy for 6022-T4 (as shown in Figs. 6 or 7a), the sensitivity of springback angle to friction coefficient was investigated. Fig. 8 shows the simulated dependence of springback angle with friction coefficient based on plane-stress calculations. The scatter in the friction coefficients is in the range of 0.02 for a single alloy [76], and 0.05 between the two uncoated materials. (The HSLA material, being coated, appears to have lower friction values.) For 6022-T4, the scatter of friction coefficient in the range of 0.02–0.05 has an effect on springback angle of a few degrees, much less than the discrepancy observed for back forces near 0.9 times the yield force.

Another possible source of error of the simulations was investigated in the guise of shell versus solid elements. Simulations were carried out using 2D solid elements (Jet2D [87]), 3D solid elements

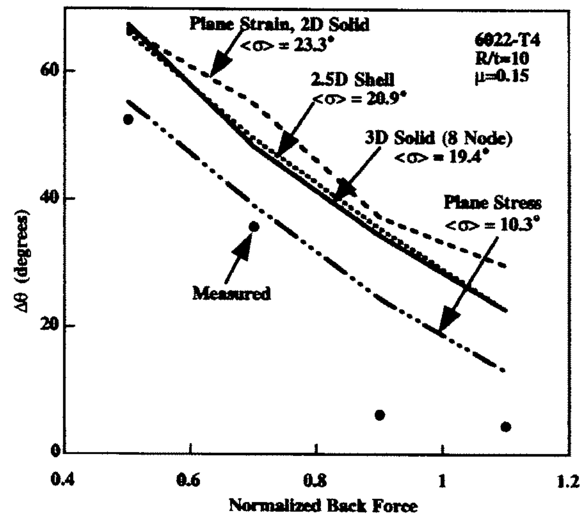

Fig. 9. Role of element choice on accuracy of springback simulation.

(C3D8R [60]), and what may be termed "2.5D shell elements". Shell calculations used meshes 300×4 in the width, and 3D solid calculations used meshes 300×4 in the half-width $\times$ 6 in the thickness. Both solid elements employed in these simulations, a four-node 2D one and an 8-node brick element, use linear shape functions. The 2.5D shell elements are in fact 4-node shell elements (S4R), with the nodes constrained to eliminate curvature outside of the plane normal to the tool axis. Thus, this simulation allows for lateral contraction during stretching, but does not allow curvature outside of the plane. The results for these choices lie in a narrow band containing the plane-strain results, Fig. 9. Thus, neither the shell formulation nor the neglect of lateral straining is a significant source of error in the 2D simulations.

When either 3D shell elements were used without constraint, or when higher-order 3D 20-node solid elements were employed (C3D20 [60]), the simulations improved markedly. Comparison of Fig. 10a and b demonstrates that the origin of the improvement lies with the *persistent anticlastic curvature**, that appears for normalized back forces greater than 0.8. For low back forces, the secondary curvature is present during forming, but nearly disappears when the specimen is unloaded. For normalized back forces greater than 0.8, the secondary curvature persists throughout the unloading, and thus presents a greater effective cross-sectional moment of inertia resisting the principal springback.

Fig. 11 compares typical 3D simulations with measurements. In view of computation time (in some cases approaching 100 h), only 6 20-node solid elements were employed through the sheet thickness. With this small number they are somewhat too stiff, although are much better than linear solid elements. In order to match the shell's 51 integration points through the thickness, an unrealistic number of solid elements would be required. Comparison of the 2D simulations and 3D simulations versus measurements (Figs. 7 and 11) shows that the only dramatic difference between 2D and 3D simulations was found for the 6022-T4 aluminum, which, being thinner, showed a larger effect.

In spite of the numerical disadvantages, solid elements are required for accuracy, when R/t ratios are lower than 5–6, Fig. 12. Under these circumstances, the assumed linear variation of strain through

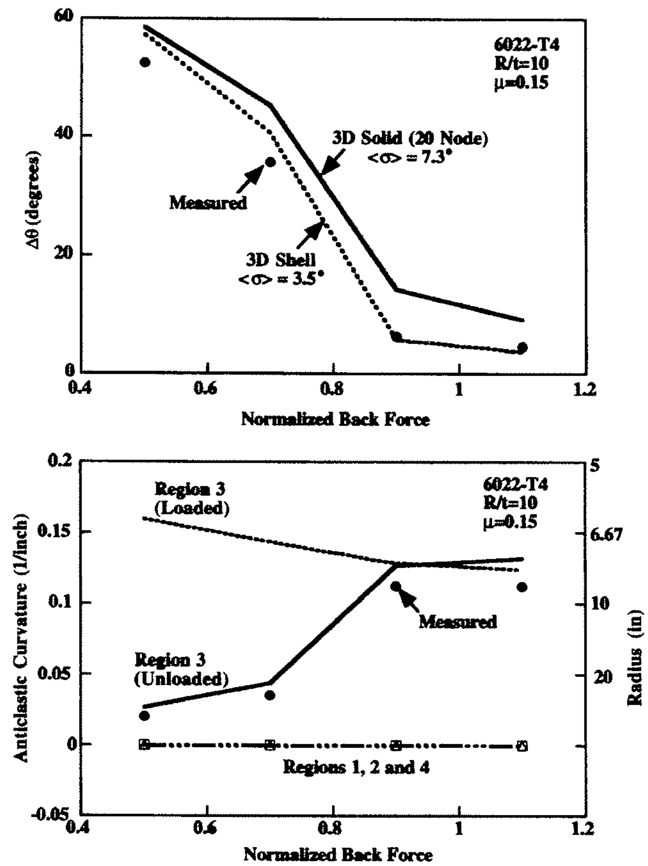

Fig. 10. Role of secondary curvature on the accuracy of springback simulation for 6022-T4 aluminum: (a) Comparison springback angles; and (b) secondary curvature.

the thickness is no longer valid, and the additional expense of using solid elements is justified (even if more approximate integration of stress through the thickness is required).

The physical effect of friction on springback angle can be now examined more realistically with shell elements (as compared to the plane-stress simulation results presented in Fig. 8). In Fig. 13, shell simulations for 6022-T4 using various friction coefficients and a normalized back force of 0.9 are compared with measurements. The trends and sensitivities are in good agreement, and the rapid drop in springback angle corresponds to the appearance of persistent anticlastic curvature as the sheet tension increases. For low values of friction coefficient, the sheet tension does not reach the yield force. As friction coefficient increases, the sheet tension of material leaving the die radius increases correspondingly, similar to an increase of back force for a constant friction coefficient (as shown, for example, in Fig. 7).

The role of plastic hardening following a strain reversal (Bauschinger effect) in simulated springback angles was investigated. As a preliminary test, measured uniaxial tension–compression results [88] for the same lot of 6022-T4 used for draw-bend tests, Fig. 14a, were fit by a simple mixed hardening law [89,90]. The hardening type is partitioned according to a parameter m ($m = 0$ for isotropic

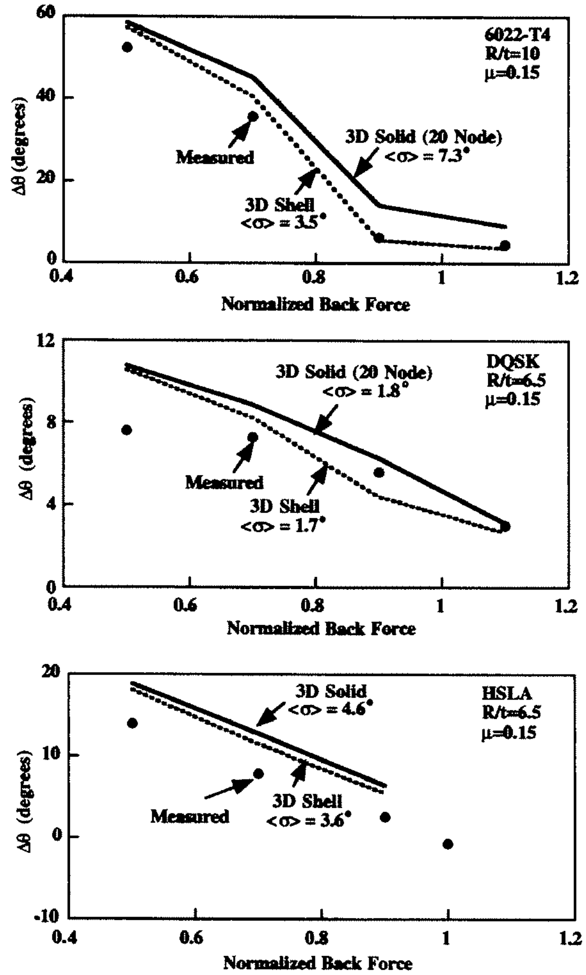

Fig. 11. Comparison of total springback angle from measurements and 3D simulations.

hardening and $m = 1$ for pure kinematic hardening of the Ziegler type [91]). It was necessary to introduce m as a function of von Mises effective plastic strain to fit the tension–compression data adequately for a single tension–compression loop, even ignoring the small-strain transient immediately following the reversal [92]. This hardening law was implemented in ABAQUS and a uniaxial tension–compression test was simulated to verify the accuracy of the constitutive equation obtained, Fig. 14a.

Fig. 14b compares simulations of the draw-bend test with and without accounting for a Bauschinger effect. The isotropic hardening simulations, as utilized for all previous simulations presented, shows a standard deviation from the experiments of 3.6°, while including the Bauschinger effect in the constitutive equation reduces the deviation to 1.8°, a 50% reduction. These results are based on fitting to only one cycle of tension–compression, at one magnitude of strain. Work to extend the constitutive model to other strains and materials is now underway. It appears likely that the Bauschinger effect, which in aluminum reduces the flow stress following a path reversal, is the cause of the pervasive over-prediction of springback angles on the basis of an isotropic hardening assumption, Figs. 9–11.

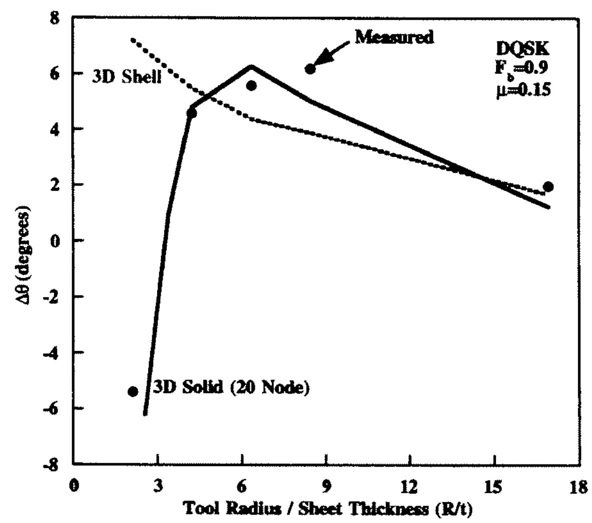

Fig. 12. Accuracy of springback simulation using shell and solid elements as function of R/t.

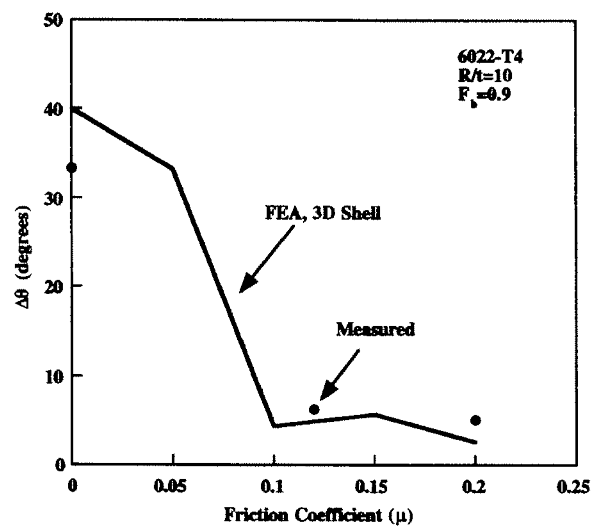

Fig. 13. Comparison of sensitivity of total springback angle to friction coefficient for 6022-T4.

4. Conclusions

Simulations of the draw/bend test over a typical range of process variables were carried out for three typical sheet alloys. The test corresponds closely to the drawing of sheet metal over a die radius into a die cavity during a typical forming operation, with springback dominated by the sidewall curl. The dependence of simulated springback on both numerical parameters and physical ones has been investigated, and, where data was available, the results have been compared with experiments presented in a companion paper.

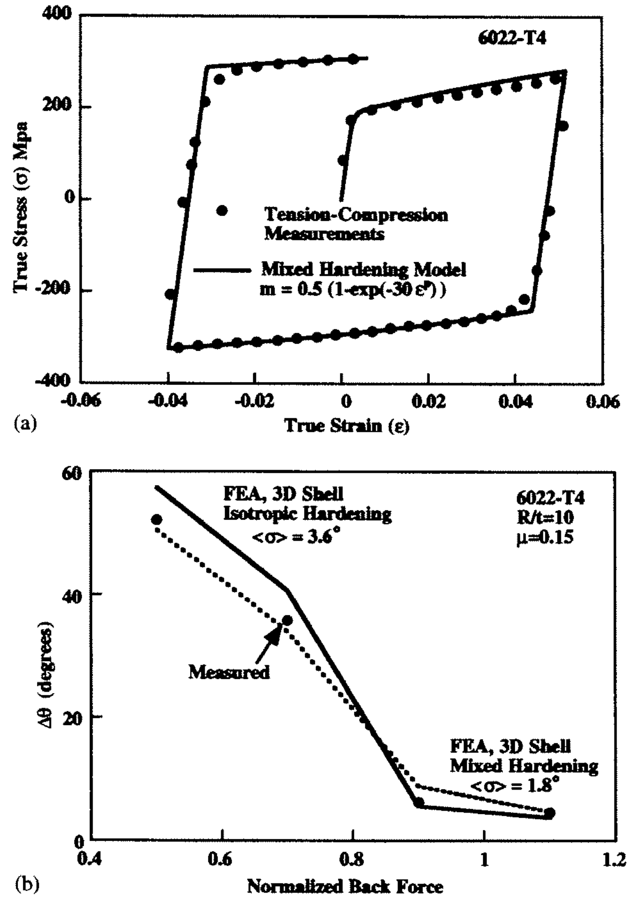

Fig. 14. Role of Bauschinger effect in draw-bend springback: (a) typical measured and simulated tension–compression hardening for 6022-T4; and (b) springback simulation results using constitutive equations with and without Bauschinger effect.

The following conclusions were reached regarding the choice of numerical parameters.

- Whereas typical forming simulations are acceptably accurate with 5–9 through-thickness integration points for shell/beam type elements [30,31], springback analysis within 1% numerical error requires up to 51 points, and more typically 15–25 points, depending on R/t, sheet tension, and friction coefficient.
- More contact nodes are necessary for springback simulation than for forming simulation, approximately one node per 5° of turn angle versus 10° recommended for forming [78]. For coarse meshes violating this guideline, the simulated springback can be of the opposite sense from physical springback.
- Equilibrium convergence and contact tolerances must be enforced carefully throughout the forming and unloading operations, but values typical of commercial implicit forming simulations are sufficient.

- 3D shell and non-linear solid elements are preferred for springback prediction even for large w/t ratios (greater than 50 in the current work) because of the presence of *persistent anticlastic curvature*.
- For R/t values greater than 5–6, current solid elements are too computation–intensive in view of the large number of points which are required through the thickness.
- For small R/t ratios (less than 5–6), nonlinear 3D solid elements are required for accurate springback predictions. This range has been reported as the division between thin shell and thick shell behavior in bending [93] and the division where bending effects become important in stretch forming operations [79]. For these high curvatures, the error involved in using a small number of nonlinear solid elements through the thickness can be less than incurred using the thin shell approximation with numerous integration points.

The following conclusions can be made regarding physical sensitivity of springback:

- The magnitude of the sheet tension during draw bending dominates other physical variables, as reported by nearly all springback studies appearing in the literature.
- The effect of friction on springback occurs principally by increasing the sheet tension. In the drawbend test, where back force can be controlled independently, the friction coefficient usually has a modest effect on springback. For metal forming operations, friction may induce larger changes in sheet tension via draw bead action and blank holder restraint.
- Persistent anticlastic curvature for the nominally two-dimensional draw-bend test leads to large discrepancies between 2-D simulations and experiments as the sheet tension approaches the yield stress, particularly for the thinner 6022-T4 aluminum alloy.
- The effect of R/t is a gradual reduction in springback for increasing R/t greater than 5 or 6. For R/t less than 5 or 6, springback is reduced rapidly for decreasing R/t, dropping to zero around $R/t = 2$.
- The presence of a Bauschinger effect alters springback angles significantly and thus must be taken into account in bending/unbending operations.

Acknowledgements

We would like to thank the National Institute of Science and Technology for an Advanced Technology Project under the auspices of PNGV, CAMMAC (Center for Advanced Materials and Manufacturing of Automotive Components) for matching funding, the Ohio Supercomputer Center for computer resources (PAS080), and Michael Wenner for many helpful discussions. Lumin Geng and Vijay Balakrishnan contributed constitutive equations incorporating the Bauschinger Effect. Chris Putnam helped construct the manuscript.

References

[1] Levy BS. Empirically derived equations for predicting springback in bending. Journal of Applied Metalworking 1984;3:135–41.

[2] Gardiner FJ. The springback of metals. Transactions of ASME 1957;79:1–9.

[3] Queener CA, De Angelis RJ. Elastic springback and residual stresses in sheet metal formed by bending. Transactions of ASM 1968;61:757–68.
[4] Shaffer BW, House Jr RN. The elastic–plastic stress distribution within a wide curved bar subjected to pure bending. ASME Journal of Applied Mechanics 1955;22:305–10.
[5] Baba A, Tozawa Y. Effect of tensile force in stretch-forming process on the springback. Bulletin of JSME 1964;7: 834–43.
[6] Ingrarson J. Residual stresses, effect on buckling. Proceedings of the Third International Special Conference on Cold Formed Steel Structure, 1975. p. 85–119.
[7] Ueda M, Ueno M, Kobayashi M. A study of springback in the stretch bending of channels. Journal of the Mechanics and Working Technology 1981;5:163–79.
[8] Yu TX, Johnson W. Influence of axial force on the elastic–plastic bending and springback of a beam. Journal of the Mechanics and Working Technology 1982;6:5–21.
[9] Yuen WYD. Springback in the stretch-bending of sheet metal with non-uniform deformation. Journal of Materials Processing Technology 1990;22:1–20.
[10] Tozawa Y. Forming technology for raising the accuracy of sheet-formed products. Journal of Materials Processing Technology 1990;22:343–51.
[11] Wang C, Kinzel G, Altan T. Mathematical modeling of plane-strain bending of sheet and plate. Journal of Materials Processing Technology 1993;39:279–304.
[12] El-Domiaty AA, Shabara MAN, Al-Ansary MD. Determination of stretch-bendability of sheet-metals. International Journal of Machine Tools Manufacturing 1996;36:5:635–50.
[13] Zhang, ZT, Hu, SJ. Mathematical modeling in plane strain bending. SAE Technical Publication No. 970439, Society of Automotive Engineers, 1997.
[14] Chan KC, Wang SH. Theoretical analysis of springback in bending of integrated circuit leadframes. International Journal of Materials Processing Technology 1999;91:111–5.
[15] Nadai A. Theory of flow and fracture of solids. New York: McGraw-Hill, 1950. p. 1.
[16] Phillips A. Introduction to plasticity. New York: Ronald Press Co., 1956.
[17] Huang M, Gerdeen JC. Springback of doubly curved developable sheet metal surface. Analysis of Autobody Stamping Technology, Society of Automotive Engineers 1994. p. 125–38.
[18] Yu TX, Zhang LC. Plastic bending, theory and applications. Singapore: World Scientific, 1996.
[19] Sudo C, Kojima M, Matsuoka T. Some investigations on elastic recovery of press formed parts of high. Proceedings of the 8th Biennial Congress of IDDRG, 1974. p. 192–202.
[20] Wang NM. Predicting the effect of die gap on flange springback. Proceedings of the 13th Congress of the IDDRG, Melbourne, Australia, 1984. p. 133–47.
[21] Thompson NE, Ellen CH. A simple theory for side-wall curl. Journal of Applied Metalworking 1995;4(1):39–42.
[22] Chu CC. Elastic–plastic springback of sheet metals subjected to complex plane strain bending histories. International Journal of Solids and Structures 1986;22:1071–81.
[23] Kuwabara T, Takahashi S, Ito K. Springback analysis of sheet metal subjected to bending–unbending under tension I (Theory and Results of Numerical Analysis). In: Altan T, editor. Advanced technology of plasticity. (Proceedings of the 5th ICTP), Columbus, Ohio, 1996, vol. II. p. 743–6.
[24] Zhang LC, Lin Z. An analytical solution to springback of sheet metals stamped by a rigid punch and an elastic die. Journal of Materials Processing Technology 1997;63:49–54.
[25] Yoshida K. Shape fixability of steel sheets in press forming. Sci. Papers. Institute of Physical and Chemical Research (RIKKEN). 1965, vol. 59. p. 87–96.
[26] Duncan JL, Bird JE. Approximate calculations for draw die forming and their applications to aluminum alloy sheet. Proceedings of the 10th Congress of the IDDRG, Warwick, England, 1978. p. 45–52.
[27] Wenner ML. On the work hardening and springback in plane strain draw forming. Journal of Applied Metalworking 1983;2:277–87.
[28] Mickalich MK, Wenner ML. Calculation of springback and its variation in channel forming operations. SAE paper 880526, in P-206. Advances and trends in automotive sheet metal stamping. Warrendale, PA: Society of Automotive Engineers, 1988. p. 99–100.
[29] Zhang ZT, Lee D. Effect of process variables and material properties on the springback of 2D-draw bending parts. SAE paper 950692, in SP-1067. Warrendale, PA: Society of Automotive Engineers, 1995. p. 11–18.

[30] Makinouchi A, Nakamachi E, Onate E, Wagoner RH, editors. NUMISHEET '93, The Institute of Physical and Chemical Research, 1993.
[31] Lee JK, Kinzel GL, Wagoner RH, editors. NUMISHEET '96, The Ohio State University, 1996.
[32] Gelin JC, Picart P, editors. Proceedings of NUMISHEET '99, University of Franche-Compte, Besancon, France, 1999.
[33] Shen SF, Dawson PR, editors. Proceedings of NUMIFORM '95. Simulation of materials processing: theory, methods and applications. Rotterdam: A.A. Balkema, 1995.
[34] Mattiasson K, Strange A, Thilderkvist P, Samuelsson A. Simulation of springback in sheet metal forming. Fifth International Conference on Numerical Methods in Industrial Forming Process, New York, 1995. p. 115–24.
[35] Wagoner RH, Carden WD, Carden WP, Matlock DK. In: Chandra T, Leclair SR, Meech JA, Verma B, Smith M, Balachandran B, editors. Springback after drawing and bending of metal sheets, Proceedings of the IPMM '97—Intelligent Processing and Manufacturing of Materials, vol. 1 (Intelligent Systems Applications). University of Wollongong, 1997. p. 1–10.
[36] Li KP, Geng LM, Wagoner RH. In: Meech JA, Veiga MM, Smith MH, LeClair SR, editors. Simulation of springback with the draw/bend test, IPMM '99. IEEE, Vancouver, BC, Canada, ISBN 0-7803-5489-3, 1999. p. 1.
[37] Lee SW, Yang DY. An assessment of numerical parameters influencing springback in explicit finite element analysis of sheet metal forming process. Journal of Materials Processing Technology 1998;80–81:60–7.
[38] Li KP, Geng L, Wagoner RH. In: Geiger M, editor. Simulation of springback: choice of element, advanced technology of plasticity 1999, vol. III. Berlin: Springer, 1999. p. 2091–8.
[39] He N, Wagoner RH. In: Lee JK, Kinzel GL, Wagoner RH, editor. Springback simulation in sheet metal forming. NUMISHEET '96, Ohio: The Ohio State University, 1996. p. 308–15.
[40] Focellese L, Fratini F, Gabrielli Micari F. The evaluation of springback in 3D stemping and coining processes. Journal of Materials Processing Technology 1998;80–81:108–12.
[41] Narasimhan N, Lovell M. Predicting springback in sheet metal forming: an explicit to implicit sequential solution procedure. Finite Elements in Analysis and Design 1999;33:29–42.
[42] Tang SC. Analysis of springback in sheet forming operation, advanced technology of plasticity. In: Lange K, editor. Advanced technology of plasticity, vol. 1. Berlin: Springer, 1987. p. 193–7.
[43] Hu Y, Du C. In: Gelin JC, Picart P, editors. Quasi static finite element algorithms for sheet metal stamping springback simulation. Proceedings of NUMISHEET '99. Besancon, France: University of Franche-Compte, 1999. p. 71–6.
[44] Geng LM, Wagoner RH. Springback analysis with a modified hardening model. Sheet Metal Forming: Sing Tang 65th Anniversary Volume, SP-1536, SAE Publication 2000-01-0768, Society of Automotive Engineers, 2000. p. 21–32.
[45] Park DW, Kang JJ, Hong JP, Oh SI. Springback simulation by combined method of explicit and implicit FEM. In: Gelin JC, Picart P, editors. Proceedings of NUMISHEET '99. Besancon, France: University of Franche-Compte, 1999. p. 35–40.
[46] Valente, Traversa D. Springback calculation of sheet metal parts after trimming and flanging. In: Gelin JC, Picart P, editors. Proceedings of NUMISHEET '99. Besancon, France: University of Franche-Compte, 1999. p. 59–64.
[47] Montmayeur N, Staub C. Springback prediction with OPTRIS. In: Gelin JC, Picart P, editors. Proceedings of NUMISHEET '99. Besancon, France: University of Franche-Compte, 1999. p. 41–46.
[48] Kazama K, Nukaga T, Makino H. Springback simulation of truck's frame side member. In: Gelin JC, Picart P, editors. Proceedings of NUMISHEET '99. Besancon, France: University of Franche-Compte, 1999. p. 65–70.
[49] Abdelsalam U, Sikorski A, Karima M. Application of one step springback for product and early process feasibility on sheet metal stampings. In: Gelin JC, Picart P, editors. Proceedings of NUMISHEET '99. Besancon, France: University of Franche-Compte, 1999. p. 47–52.
[50] Pourboghrat F, Chu E. Springback in plane strain stretch/draw sheet forming. International Journal of Mechanical Sciences 1995;36(3):327–41.
[51] Karafillis AP, Boyce MC. Tooling design in sheet metal forming using springback calculations. International Journal of Mechanical Sciences 1992;34(2):113–31.
[52] Karafillis AP, Boyce MC. Tooling design accommodating springback errors. Journal of Materials Processing Technology 1992;32:499–508.
[53] Karafillis AP, Boyce MC. Tooling and binder design for sheet metal forming processes compensating springback error. International Journal of Machine Tools and Manufacture 1996;36:503–26.

[54] Ghouati O, Joannic D, Gelin JC. Optimisation of process parameters for the control of springback in deep drawing. Simulation of materials processing: theory, methods and applications, Numiform '98, Netherlands, 1998. p. 819–24.
[55] Han SS, Park KC. An investigation of the factors influencing springback by empirical and simulative techniques. Proceedings of Numisheet'99. Besancon, France, 1999. p. 53–7.
[56] Chakhari ML, Jalinier JN. Springback of complex parts. Thirteenth Biennial Congress of IDDRG, 1984. p. 148–59.
[57] Morestin F, Boivin B. On the necessity of taking into account the variation in the Young's modulus with plastic strain in elastic–plastic software. Nuclear Engineering and Design 1996;91. 162:107–16.
[58] Tang SC. Application of an anisotropic hardening rule to springback prediction. In: Altan T, editor. Advanced technology of plasticity (Proceedings of the 5th ICTP), Columbus, Ohio, 1996, vol. II. p. 719–22.
[59] Kuwabara T, Seki N, Takahashi S. A rigorous numerical analysis of residual curvature of sheet metals subjected to bending–unbending under tension. In: Geiger M, editor. Advanced technology of plasticity, vol. II. Berlin: Springer, 1999. p. 1071–5.
[60] ABAQUS user Manual, version 5.7 or recently 5.8.14.
[61] Wagoner RH, Wang CT, Nakamachi E. Quick analysis of sheet forming using sectional FEM. Proceedings of the First Japan International SAMPE, Symposium Exhibition, SAMPE, 1989. p. 695–700.
[62] Wang CT, Wagoner RH, Square-punch forming: section analysis and bending study (SAE paper no. 910772), Autobody stamping technology progress. Soc. Auto. Engrs., SP-865, Warrendale, Pennsylvania, 1991. p. 119–27.
[63] Wang CT, Wagoner RH. Plane-strain deep drawing: finite element modeling and measurements (SAE paper no. 910774), Autobody stamping technology progress. Soc. Auto. Engrs., SP-865, Warrendale, Pennsylvania, 1991. p. 133–42.
[64] Saran MJ, Keum YT, Wagoner RH. Section analysis with irregular tools and arbitrary draw-in conditions for numerical simulation of sheet forming. International Journal of Mechanical Sciences 1991;33:893–910.
[65] Keum YT, Saran MJ, Wagoner RH. Practical die design via section analysis. Journal of Materials Processing Technology 1992;35:1–36.
[66] Germain Y, Chung K, Wagoner RH. A rigid-visco-plastic finite element program for sheet metal analysis. International Journal of Mechanical Sciences 1989;31:1–24.
[67] Keum YT, Nakamachi E, Wagoner RH, Lee JK. Compatible description of tool surfaces and FEM meshes for analyzing sheet forming operations. In: Thompson EG, Wood RD, Zienkiewicz OC, Samuelsson A, editors. NUMIFORM '89-numerical methods in industrial forming processes. Rotterdam: Balkema, 1989. p. 489–496.
[68] Wagoner RH, Kim YH, Keum YT. 3-D sheet forming analysis including the effects of strain hardening, rate sensitivity, anisotropy, friction, heat generation, and transfer. Advanced technology of plasticity. Japan Society of Technology of Plasticity, 1990. p. 1751–6.
[69] Kim YH, Wagoner RH. A 3-D finite element method for non-isothermal sheet forming processes. International Journal of Mechanical Sciences 1991;33:911–26.
[70] Wagoner RH, Zhou D. Analyzing sheet forming operations—recent numerical and experimental advances. In: Chenot J-L, Wood RD, Zienkiewicz OC, editors. Numerical methods in industrial forming processes—NUMIFORM '92. Rotterdam: A.A. Balkema, 1992. p. 123–32.
[71] Wagoner RH, Zhou D. Recent advances in 3-D numerical simulation of sheet forming operations. In: Wang ZR, Yuxin He, editors. Advanced technology of plasticity—1993. Beijing: Int. Academic Publ., 1993. p. 1747–55.
[72] Zhou D, Wagoner RH. Development and application of sheet forming simulation. Journal of Materials Processing Technology 1995;50:1–16.
[73] Saran MJ, Wagoner RH. A consistent implicit formulation for nonlinear finite element modeling with contact and friction, Part 1—Theory. ASME Transactions, Journal of Applied Mechanics 1991;58:499–506.
[74] Saran MJ, Wagoner RH. A consistent implicit formulation for nonlinear finite element modeling with contact and friction, Part 2—numerical verification and results. ASME Transactions, Journal of Applied Mechanics 1991;58: 507–12.
[75] Zhou D, Wagoner RH. An N-CFS algorithm for sheet forming FE modeling, metal forming process simulation in industry, vol. II. Monchengladbach, Germany: Druckerei GmbH, 1994. p. 57–74.
[76] Carden W, Geng LM, Matlock DK, Wagoner RH. Measurement of springback. International Journal of Mechanical Sciences 2002;44:79–101.
[77] Li KP, Wagoner RH. Simulation of springback. In: Huetink J, Baaijens F.P.T, editors. Simulation of Materials Processing. Rotterdam: A.A. Balkema, 1998. p. 21–32.

[78] Frey WH, Wenner ML. Development and application of a one-dimensional finite element code for sheet metal forming. In: Samanta SK, Komanduri D, McMeeking R, Chen MN, Tseng A, editors. Interdisciplinary issues in material processing and manufacturing. New York: ASME, 1987. p. 307–19.
[79] Wang NM, Tang SC. Analysis of bending effects in sheet metal forming operations. International Journal for Numerical Methods in Engineering 1988;25:253–67.
[80] Joannic D, Gelin JC. Shape defects in sheet metal forming operations after springback. NUMISHEET '99. 1999. p. 29–34.
[81] Wang CT, Kinzel G, Altan T. Mechanical modeling of plane-strain bending of sheet and plate. Journal of Materials Processing Technology 1993;39:279–304.
[82] Hosford, Caddell R. Metal forming: mechanics and metallurgy. Englewood Cliffs, NJ: Prentice-Hall, 1993.
[83] Burgoyne CJ, Crisfield MA. Numerical integration strategy for plates and shells. International Journal for Numerical Methods in Engineering 1990;29:105–21.
[84] I-Nan, Chou, Hung C. Finite element analysis and optimization on springback reduction. International Journal of Machine Tools and Manufacture 1999;39:517–36.
[85] Park DW, Kang JJ, Hong JP, Oh SI. Springback simulation by combined method of explicit and implicit FEM. NUMISHEET '99. 1999. p. 35–40.
[86] Horrocks D, Johnson W. On anticlastic curvature with special reference to plastic bending: a literature survey and some experimental investigations. International Journal of Mechanical Sciences 1967;8:835–61.
[87] Jetteur P, Cescotto S. A mixed finite element for the analysis of large inelastic strains. International Journal for Numerical Methods in Engineering 1991;31:229–39.
[88] Balakrishnan V. Measurement of in-plane Bauschinger effect in metal sheets. Masters thesis, The Ohio State University, Ohio, 1999.
[89] Hodge PG. A new method of analyzing stresses and strains in work hardening plastic solids. Journal of Applied Mechanics 1957;24:482–3.
[90] Prager W. A new method of analyzing stresses and strains in work hardening plastic solids. Journal of Applied Mechanics 1956;23:493–6.
[91] Ziegler H. A modification of Prager's hardening rule. Quarternery Applied Mathematics 1959;17:55–65.
[92] Geng LM. Application of plastic anisotropy and non-isotropic hardening to springback prediction. Ph.D. thesis, The Ohio State University, Ohio, June 2000.
[93] Hill R. The mathematical theory of plasticity. Oxford: Oxford University Press, 1951.
[94] Proceedings of the Sixth International Conference on Numerical Methods in Industrial Forming Processes NUMIFORM '98—Simulation of Materials Processing: Theory, Methods and Applications, 1998.